THE EFFECT OF *OsABC1K3* MUTATION ON AGRONOMIC PRODUCTIVITY AND ENZYME ACTIVITIES IN RICE

BAI, J. P. – NOOR, H. – MIN, S.*

School of Agriculture, Shanxi Agricultural University, Shanxi, China

**Corresponding author*
e-mail: sm_sunmin@126.com

(Received 23rd Jul 2025; accepted 2nd Oct 2025)

Abstract. Chloroplasts convert light energy into chemical energy and are sites of plant photosynthesis, providing energy sources for plant growth and development. The main research results were as follows: the *OsABC1K3* mutant showed intermittent chlorosis phenotype, uneven distribution of chlorophyll, and destruction of chloroplast structure in the yellow part of leaves. The *OsABC1K3* mutant was found to have significantly increased expression. TUNEL assay results showed apoptosis in the leaves of mutant *OsABC1K3*. The mutant *OsABC1K3* showed significantly increased superoxide dismutase (SOD), peroxidase (POD), and catalase (CAT) activities but failed to eliminate excess reactive oxygen species (ROS). Compared with the wild-type SN9816, the *OsABC1K3* mutant showed a significant decrease in photosynthetic performance and a decrease in half-saturating light intensity, proving that the *OsABC1K3* mutant was less adaptive to supersaturated light intensity. The activities of CAT and POD in the leaves significantly increased, which could reduce the level of ROS accumulation in the plants. The decrease in pigment content in *OsCRS2* mutant reduced the absorption of supersaturated light energy and significantly improved the utilization efficiency of light energy.
Keywords: *chlorophyll fluorescence, photosynthetic capacity, antioxidant system; yield*

Introduction

Rice (Oryza sativa L.) is a basic food crop for most of the world's population, and its yield is critical to global food security (Zhang et al., 2020). However, rice production is threatened by a variety of abiotic stresses that disrupt key physiological processes such as photosynthesis (Xu et al., 2021). Chlorophyll biosynthesis and chloroplast development are central to photosynthetic efficiency, and mutations affecting these processes often manifest as visible leaf color phenotypes (Rao et al., 2019). Although more than 100 leaf color mutation loci have been mapped in rice and more than 40 related genes have been cloned, including more than 10 chlorina genes that regulate chloroplast biosynthesis (Lin et al., 2022), such as osabc1k2, OsABC1K3, and OsHAP3C (Cui et al., 2021), the specific physiological and molecular functions of many genes remain unclear. The chlorophyll biosynthetic pathway is a critical factor for vulnerability. The process involves the tetrapyrrole pathway, where the accumulation of highly photoreactive intermediate metabolites leads to the excess production of reactive oxygen species (ROS) (Busch et al., 2015; Zhao et al., 2022). The ROS burst may cause photodynamic damage and necrotic plaques; therefore, precise regulation of this pathway is required to prevent spontaneous damage (Ma et al., 2020). To mitigate such damage, plants have evolved complex antioxidant systems, including superoxide dismutase (SOD), which converts superoxide anions to hydrogen peroxide (Rühle et al., 2021), catalase (CAT), and ascorbic acid peroxidase (APX), which scavenge ROS and maintain cellular redox homeostasis (Shikanai et al., 1999; Schöttler et al., 2017; Noctor et al., 2018). Thus, a balance between chlorophyll metabolism and antioxidant systems is essential for plant survival, especially under stress conditions that interfere with photosynthetic electron transport (Henras et al.,

http://www.aloki.hu ● ISSN 1589 1623 (Print) ● ISSN 1785 0037 (Online)
DOI: http://dx.doi.org/10.15666/aeer/2306_1115311167

2015). This balance is particularly critical in chloroplasts, which are key photosynthetic organelles of photosynthesis (Zhang et al., 2018). Under stressful conditions, the balance between ROS production and clearance is disrupted, resulting in enzyme inactivation and cell death (Niazian et al., 2021; Nikkanen et al., 2019). Changes in photosynthetic efficiency can be sensitively monitored using chlorophyll fluorescence parameters, which reflect the energy conversion processes (Nishikawa et al., 2012; Hu et al., 2018). For example, under high light conditions, non-photochemical quenching (NPQ) is activated to dissipate excess light energy and reduce ROS levels (Zhou et al., 2007). Mutants with impaired processes, such as pgr5, exhibit lower CO_2 assimilation rates and electron transport fluxes (Kumar et al., 2009), highlighting the association between photosynthetic performance and stress tolerance (He et al., 2020). Although multiple chlorine genes have been identified, there is still a significant lack of understanding of how specific mutations disrupt the delicate balance between light capture, energy conversion, and ROS management (Zhang et al., 2019).

The specific physiological consequences of mutants, such as OsABC1K3 and OsCRS2, and their compensation mechanisms are unclear. Clarifying these mechanisms is critical for filling the knowledge gap between genetic mutations and their phenotypic effects. Therefore, this study aimed to systematically characterize two chlorophyll-deficient rice mutants: intermittent chlorosis mutant OsABC1K3 and low chlorophyll mutant OsCRS2. Specific objectives include the analysis of key physiological parameters, such as chlorophyll metabolism, photosynthetic performance, and chlorophyll fluorescence characteristics, to clarify the physiological basis of mutant phenotypes, identification of causal mutations leading to phenotypes by map cloning, and preliminary functional analysis of identified genes to explore their role in chloroplast development and ROS homeostasis. This study lays a foundation for understanding the molecular mechanism of chlorophyll metabolism and oxidative stress regulation in rice, and has potential significance for breeding stress-resistant crop varieties.

Study materials and cultivation

Plant materials and culture conditions

The wild type was planted in the southern field of the Rice Research Institute of Shenyang Agricultural University, while the F2 population was planted in the Experimental Station of Shenyang Agricultural University. The seedlings were cultivated in the experimental base of the Rice Research Institute of Shenyang Agricultural University in mid-April using heat preservation and drought cultivation technology. Wild type (rice subspecies Nipponbare) and two mutants (OsABC1K3 and OsCRS2) were sterilized and germinated at 28℃. Seedlings were grown in controlled environment growth chambers (Model PGV-36, Conviron, Canada) was grown in hydroponics with a photoperiod of 14/10 h (light/dark), light intensity of 500 μmol photons·m²·s $, day and night temperatures of 28/25℃, and relative humidity of 60%, 70%. The hydroponics were modified Yoshida nutrient solution, which was changed once per week. All the physiological and molecular analyses were performed under the optimal stress-free conditions described above. At least three independent biological replicates were set up for each experiment and each replicate consisted of a mixture of tissues from three different plants. Technical replicates were performed according to the experimental requirements (e.g., multiple measurements for each leaf sample). Seedbed soil was selected as a biochar seedling substrate and transplanted after 30 d.

http://www.aloki.hu ● ISSN 1589 1623 (Print) ● ISSN 1785 0037 (Online)
DOI: http://dx.doi.org/10.15666/aeer/2306_1115311167

Instruments and manufacturers

The key instruments were used in the experiment include: UV-2600 spectrophotometer (Shimadzu Corporation, Japan) for chlorophyll content analysis; LI-6800 portable photosynthesis measurement system (LI-CORBiosciences, USA) for gas exchange parameter determination; Imaging-PAMM series chlorophyll fluorescence imaging system (HeinzWalz GmbH, Germany) for chlorophyll fluorescence parameter collection; HitachiHT7800 transmission electron microscope (Hitachi High-tech Co., Ltd., Japan) for ultrastructural observation.

Introduction to test materials

The OsABC1K3 was derived from the mutant library of Shennong 9816 (SN9816), which had been identified and selected by previous researchers for many years. SN9816 and mutant OsABC1K3, and the segregation ratio of traits was investigated when segregated phenotypes appeared in the F2 generation population (*Table 1*).

Table 1. *O_2^- reagent system*

Reagent name	Blank control tube (ml)	Measuring tube (ml)
Sample	0	0.2
Extract liquid	0.5	0.3
Reagent 1	0.4	0.4
Reagent II	Mix well in a 37°C water bath 20 min 0.3	0.3
Reagent III	Mix well in a 37°C water bath 20 min 0.3	0.3
Reagent IV	0.5	0.5

Phenotypic trait measurement

Plant architectural traits, including plant height, blade length, and panicle length, width SN9816 and mutant OsABC1K3 were measured at the mature stage on five randomly selected plants from each plot. Blade length was measured from the ligule to the tip of the flag leaf. All measurements are presented in centimeters (cm).

Investigation of agronomic traits

The full panicle stage, plant height and leaf length and width SN9816 and mutant *OsABC1K3*. After the rice panicles were allowed to air dry, yield traits such as panicle weight, panicle length, number of primary branches, number of secondary branches, number of grain and grain weight were measured.

Chlorophyll content

At the tillering and heading stages, fresh leaves of mutant *OsABC1K3* were collected, the main veins were removed, and the leaves were cut into small pieces. The centrifuge tubes were immersed in the environment for 36-48 h, during which they were shaken upside down every 8 h. After the pigment in the leaves was completely dissolved, the absorbance values at wavelengths of 646 nm was measured using a spectrophotometer. Three biological replicates were performed, and t-tests were performed using the SPSS software.

http://www.aloki.hu ● ISSN 1589 1623 (Print) ● ISSN 1785 0037 (Online)
DOI: http://dx.doi.org/10.15666/aeer/2306_1115311167

Malondialdehyde

A sample (0.5 g) was placed in a mortar with 5 mL of trichloroacetic acid (TCA) at a concentration of 5%. After full grinding, the homogenate was transferred to a centrifuge tube and centrifuged at 5000 g for 20 min at 4°C. 1.5 mL of the supernatant was aspirated and added with 0.5% thiobarbituric acid 2.5 mL of 5% TCA solution was thoroughly mixed and the reaction solution was boiled in water for 15 min, after which it was quickly cooled in an ice bath and at 4 ° cells were centrifuged at 5000 g for 10 min. The reaction solution was measured at 532 nm using a UV spectrophotometer, with distilled water as a control, the absorbance value at a wavelength of 600 nm, and the malondialdehyde concentration content of the material formula. Calculation formula:

$$\text{MDA content (nmol}\cdot\text{g}^{-1}) = [(A532 - A600) \times T \times V/a] / (1.55 \times 10^{-1} \times W) \quad \text{(Eq.1)}$$

where T represents the total volume of the reaction solution (4 mL), V is the total volume of the extract used (5 mL), a is the volume of the extraction liquid used in the water bath reaction (1.5 mL), and W represents the fresh weight (0.5 g) of the material used in the test.

Antioxidant enzyme activity

Superoxide dismutase (SOD), peroxidase (POD), and catalase (CAT) levels were measured using Solebo's activity detection kits. 0.1 g of the sample was required for each assay, and the activity was determined by UV spectrophotometry.

Photosynthetic characteristic parameters

The *OsABC1K3* was measured using the *CIRAS-3* photosynthesis apparatus in a cloud-free morning (9:00-11:00). The LED light source in the CO_2 required for photosynthesis was injected into the leaf chamber by a cylinder through a CO_2 jet system, and the CO_2 concentration was set to 390 ppm. Ten plants of consistent growth were selected for each material, and fully expanded leaves at the highest position were selected.

Determination of chlorophyll fluorescence parameters

Ten plants with the same growth of each material were selected, and the parameters were measured in the morning (9:00-10:00 am) in sunny weather, avoiding the main leaf veins.

Histological staining

Positive detection was conducted on the transgenic plants obtained through genetic transformation. The lines with ampicillin tags in the genome were cultivated and harvested. In the T1 generation, the seedlings, leaves, stems, and ears of the transgenic plants were collected and placed in 50 mL centrifuge tubes. An appropriate amount of staining solution was added and the tubes were stored in the dark. After thorough staining, tissue samples were placed in centrifuge tubes containing anhydrous ethanol for decolorization. After all chlorophyll had faded, the samples were observed and photographed.

Yield determination the mature stage (MS)

Eight holes were sampled for each treatment according to the average number of stems, and the number of panicles, number of grains per panicle, seed-setting rate, 1000-grain weight, and yield were measured. The formula used is as follows:

http://www.aloki.hu ● ISSN 1589 1623 (Print) ● ISSN 1785 0037 (Online)
DOI: http://dx.doi.org/10.15666/aeer/2306_1115311167

$$\text{Seed setting rate} = \text{number of solid seeds} / (\text{number of solid seeds} + \text{number of empty seeds} + \text{number of empty seeds}) \times 100$$

$$\text{grain weight} = \text{weight of kernels} / \text{number of kernels} \times 1000 \quad \text{(Eq.2)}$$

$$\text{1000-Yield} = \text{number of panicles} \times \text{number of kernels per panicle} \times \text{seed setting rate} \times \text{1000-grain weight} \quad \text{(Eq.3)}$$

Ultrastructural observation

Approximately 30 days after seeding, young leaves of wild-type *SN9816* and *OsABC1K3* mutants were selected, cut into approximately 0.5 cm2 pieces, and placed in 2.5% glutaraldehyde and 2% osmic acid solution for fixation. Sample sections were prepared using an ultrathin sectioning mechanism and chloroplast ultrastructure.

Statistical analysis of data

Based on t-test, SPSS22.0 software was used to compare the differences between the two groups of data of wild type and mutant at the significance level, and to analyze the statistically significant differences of all data. All data were statistically analyzed using Microsoft Excel 2021 (Microsoft Corporation, Washington, DC, USA) and GraphPad Prism 5 (v5.01) (GraphPad Software, Inc., San Diego, CA, USA). Student's t-test was conducted to compare the wild type and the ygl19 mutant, and *, ** represent significant differences at the 0.05, 0.005 levels, respectively. GraphPad Prism 5 was used to construct graphs.

Results

Phenotypic analysis of mutant OsABC1K3

At seedling stage, *OsABC1K3* mutant exhibited an intermittent green loss phenotype with yellow and green leaves (*Fig. 1a*). At the tiller-stage, the interrupted chlorosis phenotype of mutant *OsABC1K3* was most prominent (*Fig. 1 b, c, d*). After that, the new leaves of mutant *OsABC1K3* all showed a normal green color, which was not significantly different from that of SN9816 (*Fig. 1e*).

Reactive oxygen species and protective enzyme activity analysis

Leaves of wild-type SN9816 and mutant *OsABC1K3* plants were stained with DAB and NBT to reflect the level of oxidative stress in plant pairs. In DAB staining, mutant OsABC1K3 showed significantly more dark red spots on the leaves than wild-type SN9816 (*Fig. 2a*). In NBT staining, the presence of blue material on the leaves of mutant peroxide-anion OsABC1K3 was 4.5-fold higher than that of SN9816 (*Fig. 2e*), and excessive ROS caused damage to the mesophyll cells and destroyed proteins in the nucleus. To cope with high peroxidation stress, plants need a series of protective enzymes to remove reactive oxygen species (ROS). Compared with the wild type SN9816, the superoxide dismutase (SOD), peroxidase (POD), and catalase (CAT) of *OsABC1K3* mutant were increased by 30%, 153.9%, and 31.3%, respectively (*Fig. 2f, g, h*), and the differences were all extremely significant. These results suggest that chloroplast damage in *OsABC1K3* might be due to the excessive accumulation of ROS, which resulted in the peroxidation of cell lipids, and the scavenging system of the plant itself was not sufficient to completely remove the excess ROS.

http://www.aloki.hu ● ISSN 1589 1623 (Print) ● ISSN 1785 0037 (Online)
DOI: http://dx.doi.org/10.15666/aeer/2306_1115311167

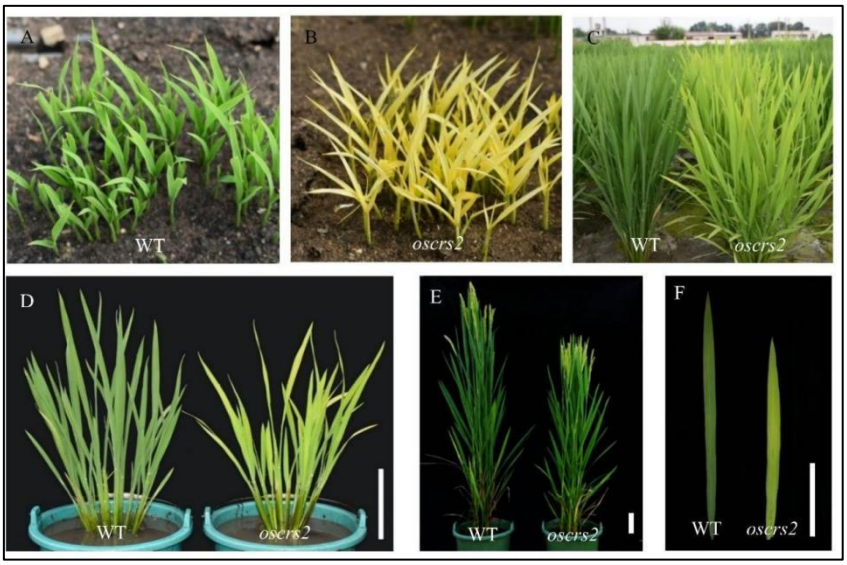

Figure 1. *Phenotype characterization of WT and OsABC1K3. (A-C) Phenotypes of WT and OsABC1K3 at the seedling stage (25 DAS) (A), the tiller stage (75 DAS) (B) and the late tillering stage (90 DAS) (C). (D) Leaves of WT and OsABC1K3 during the tillering stage. (E) Phenotypes of WT and OsABC1K3 at the full-heading stage (110 DAS)*

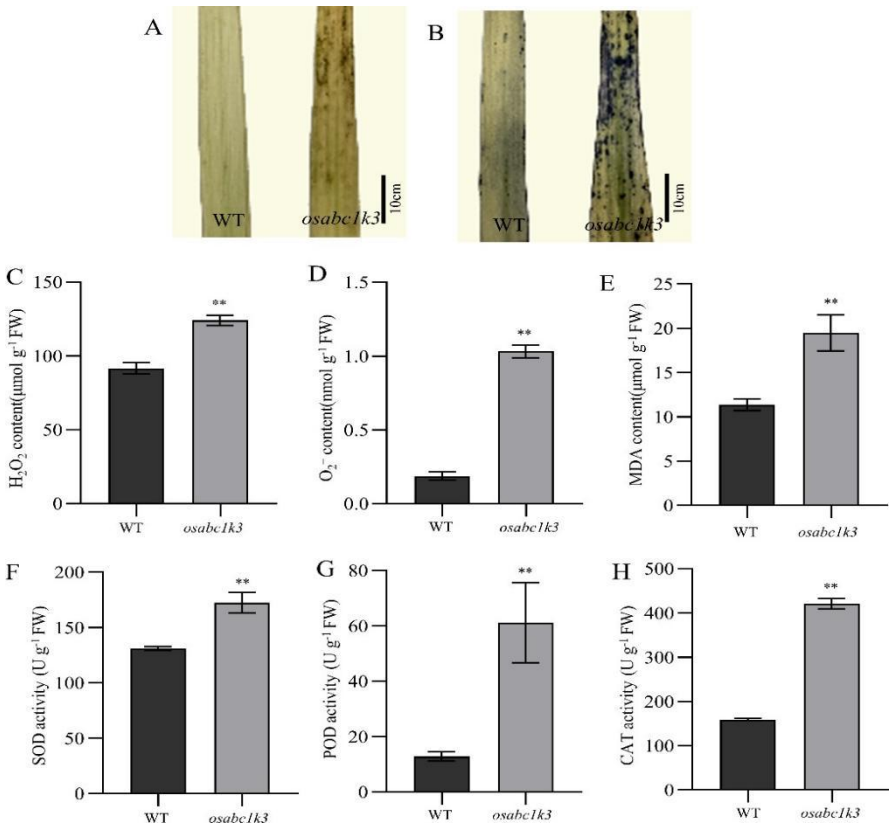

Figure 2. *ROS-related index assay in the WT and OsABC1K3. (A) DAB staining of leaves between the WT and OsABC1K3. (B) NBT staining of leaves. (C) H2O2 content. (D) Superoxide anion (O-) content. (E) MDA content. (F) SOD activity. (G) POD activity. (H) CAT activity. The Error bars indicate means ± SDs of 3 independent replicates, * represents a significant difference at the 0.05 level, ** extremely at the 0.01 level (Student's t - test)*

http://www.aloki.hu ● ISSN 1589 1623 (Print) ● ISSN 1785 0037 (Online)
DOI: http://dx.doi.org/10.15666/aeer/2306_1115311167

TUNEL analysis

The nuclear blue fluorescence signal was observed in mutant OsABC1K3, and the green fluorescence signal was significantly higher in *OsABC1K3* mutant leaves than in wild-type SN9816 leaves, indicating that a large number of DNA breaks occurred *OsABC1K3* mutant cells. It causes apoptosis (*Fig. 3*).

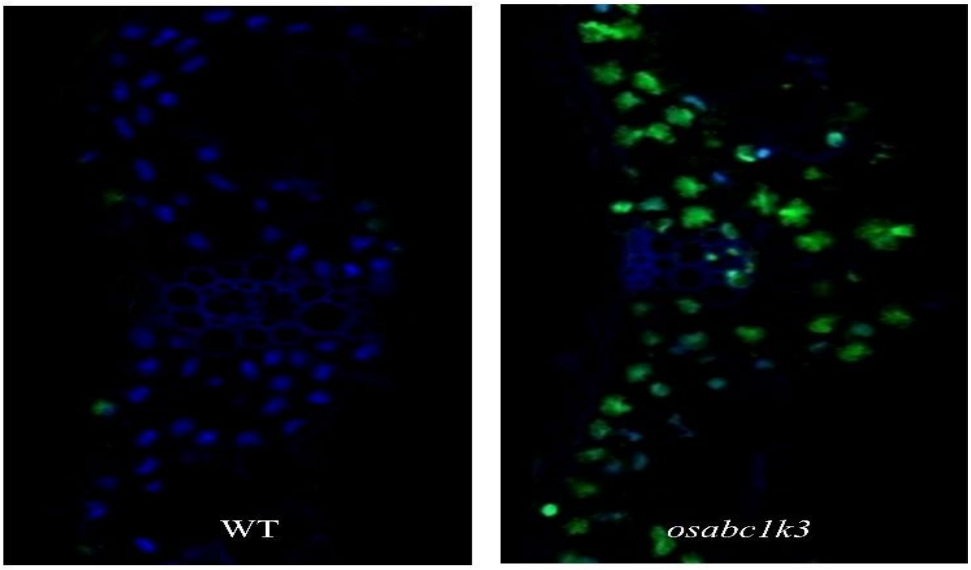

Figure 3. *TUNEL analysis of WT and OsABC1K3 leaves. Blue fluorescence is DAPI staining, green fluorescence represents positive results*

Chlorophyll fluorescence parameters

ΦPSII and Fv'/Fm' of *OsABC1K3* mutant were significantly decreased compared with those of the wild-type SN9816 (*Fig. 4*). ΦPSII represents the reagent photochemical efficiency of PSII, and Fv '/Fm' is the primary light energy capture efficiency of the reaction center of PSII. This decrease indicated that the photosynthetic efficiency of the mutant *OsABC1K3* was significantly inhibited.

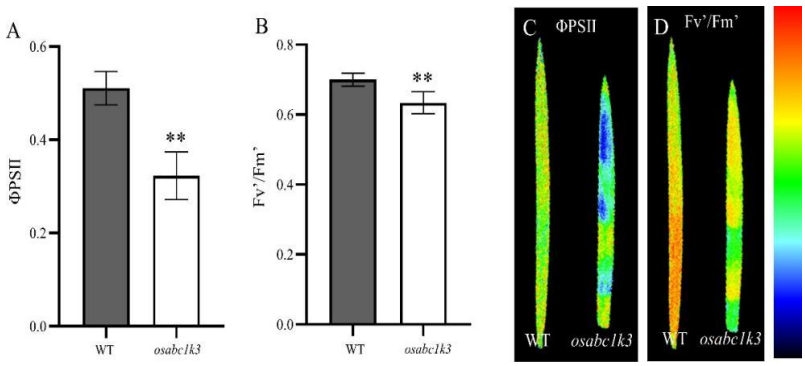

Figure 4. *Chlorophyll fluorescence parameters in WT and OsABC1K3. (A-B) Variations in the ΦPSII (A) Fv'/Fm' (B). (C-D) Chlorophyll fluorescence image. The error bars indicate means ± SDs of 3 independent replicates, * represents a significant difference at the 0.05 level, ** extremely at the 0.01 level (Student's t - test)*

http://www.aloki.hu ● ISSN 1589 1623 (Print) ● ISSN 1785 0037 (Online)
DOI: http://dx.doi.org/10.15666/aeer/2306_1115311167

Compared with the wild-type SN9816, the Fv/Fm ratio of *OsCRS2* mutant was not significantly different, but the actual photochemical quenching (NPQ) was reduced by 15.3% (*Fig. 5a, b, c, d*). The chlorophyll fluorescence imaging results were consistent with the above results (*Fig. 5e*). The higher ΦPSII of *OsCRS2* indicated that its carbon assimilation potential was improved, and the significantly increased qP indicated that the PSII opening degree of *OsCRS2* was higher. Therefore, the abnormal pigment content of *OsCRS2* mutant affects leaf color.

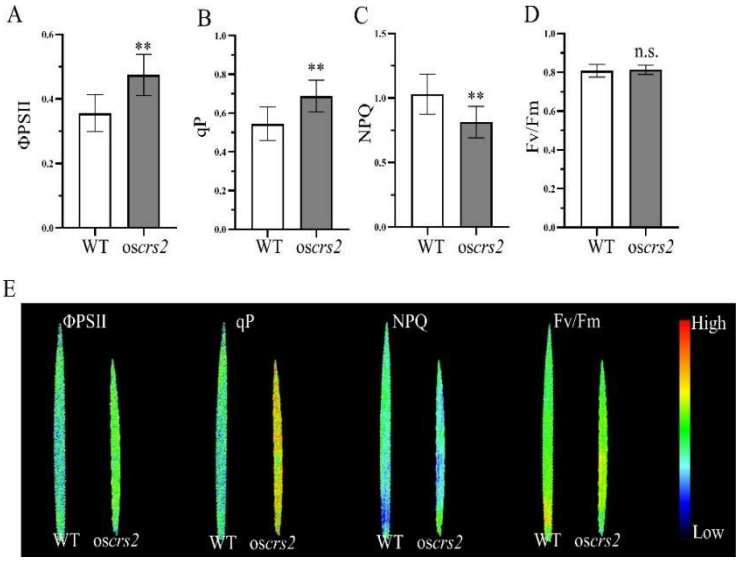

Figure 5. *Fluorescence parameters of the WT and OsCRS2. (A-D) Variations in the ΦPSII (A), qP (B), NPQ (C) and Fv/Fm (D). (E) Chlorophyll fluorescence image. The error bars indicate means ± SDs of 3 independent replicates, * represents a significant difference at the 0.05 level, ** extremely at the 0.01 level (Student's t - test)*

Agronomic traits

The average plant height of mutant OsABC1K3 decreased by 7.8% and 16.8% in 2020 and 2021, respectively, A highly significant difference (*Fig. 6a*). Blade length SN9816 and *OsABC1K3* mutant was no significant (*Fig. 6b, c*). In terms of yield traits, compared with the wild type SN9816, the spike length, spike weight, secondary branch number and seed setting rate of OsABC1K3 mutant decreased significantly in 2020 and 2021, while the primary branch number and 1000-grain weight showed no significant difference. Spike length and panicle weight in mutants are consistently lower than in wild types across both years, with significant differences in both years. The number of secondary branches and seed setting rate also show significant decreases in mutants in both years (*Table 2*). Spike length (cm) 2020: WT = 17.92 ± 1.17, Mutants = 16.04 ± 1.14 significant decrease in mutants 2021: WT = 17.94 ± 1.05, Mutants = 15.84 ± 1.1, another significant decrease in mutants. Panicle weight (g) 2020: WT = 3.62 ± 0.62, Mutants = 3.14 ± 0.66 significant decrease in mutants 2021: WT = 3.64 ± 0.69, Mutants = 3.18 ± 0.69 (another significant decrease in mutants. Number of secondary branches 2020: WT = 24.32 ± 7.12, Mutants = 18.23 ± 6.1 significant decrease in mutants 2021: WT = 26.3 ± 6.31, Mutants = 20.4 ± 6.07 (another significant decrease in mutants. Seed setting rate (%) 2020: WT = 94.41 ± 1.51, Mutants = 89.18 ± 3.24 significant decrease in mutants 2021: WT = 92.37 ± 1.52, Mutants = 85.45 ± 2.16 (another significant decrease in mutants).

http://www.aloki.hu ● ISSN 1589 1623 (Print) ● ISSN 1785 0037 (Online)
DOI: http://dx.doi.org/10.15666/aeer/2306_1115311167

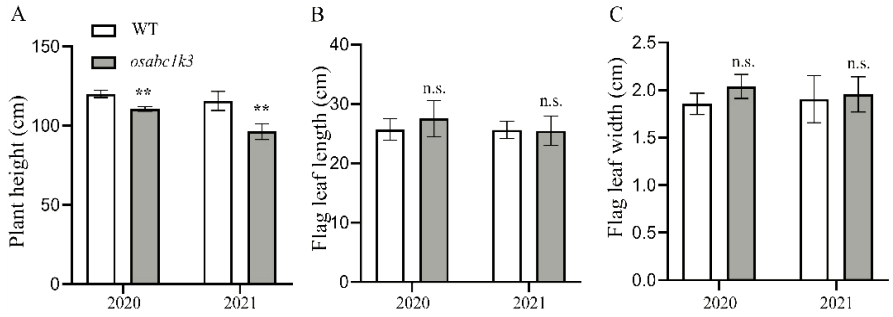

Figure 6. *Agronomic characters of WT and OsABC1K3. (A) Plant height of WT and OsABC1K3; (B) Flag leaf length; (C) Flag leaf width. * indicates a significant difference at the 0.05 level and ** indicates a very significant difference at the 0.01 level (student's t-test)*

Table 2. *Agronomic characters of WT and OsABC1K3*

Characters	Year	Wild type (WT)	Mutants *OsABC1K3*
Spike length (cm)	2020	17.92 ± 1.17	16.04 ± 1.14 **
	2021	17.94 ± 1.05	15.84 ± 1.1 **
Panicle weight (g)	2020	3.62 ± 0.62	3.14 ± 0.66 **
	2021	3.64 ± 0.69	3.18 ± 0.69 **
Number of panicles	2020	10.1 ± 1.1	9.8 ± 1.1
	2021	9.5 ± 1.5	9.4 ± 1.6
Number of branches at a time	2020	13.45 ± 1.14	13.68 ± 1.47
	2021	13.74 ± 1.31	12.9 ± 1.08
Number of secondary branches	2020	24.32 ± 7.12	18.23 ± 6.1 **
	2021	26.3 ± 6.31	20.4 ± 6.07 **
Seed setting rate (%)	2020	94.41 ± 1.51	89.18 ± 3.24 **
	2021	92.37 ± 1.52	85.45 ± 2.16**
1000-grain weight (g)	2020	24.67 ± 0.96	25.32 ± 1.2
	2021	24.15 ± 1.02	24.33 ± 0.73

* ($p < 0.05$) and ** ($p < 0.01$) indicate significant differences between WT and *OsABC1K3*. The *OsABC1K3* mutation negatively impacts spike development, panicle weight, branching complexity, and fertility, but does not affect grain size or primary panicle architecture. The consistency across two years strengthens the reliability of these findings

Expression pattern of OsCRS2

OsCRS2 is expressed in all aboveground parts of the plant. The parts with the highest expression levels were the young leaves, followed by the mature leaves. However, *OsCRS2* expression was barely detected in the roots (*Fig. 7A*). Through genetic transformation, the GUS gene was inserted into wild-type rice plants and the expression of the GUS gene was driven by the *OsCRS2*. Tissue staining was performed on the transgenic plants, and GUS expression was detected in the leaves, stems, leaf sheaths, and ears. These results were consistent with the *qRT-PCR* results (*Fig. 7B, C, D, E*).

http://www.aloki.hu ● ISSN 1589 1623 (Print) ● ISSN 1785 0037 (Online)
DOI: http://dx.doi.org/10.15666/aeer/2306_1115311167

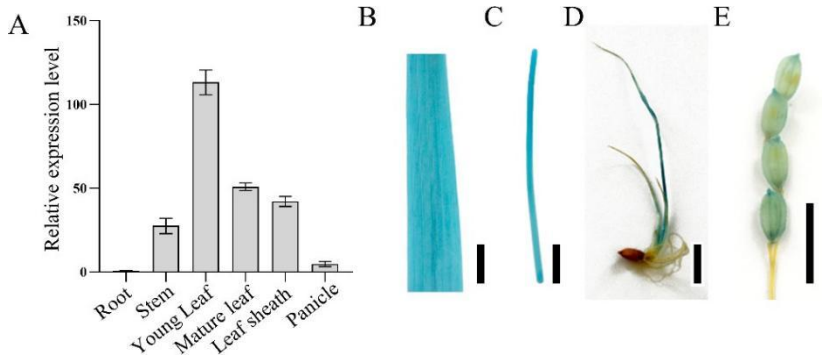

Figure 7. *Tissue expression pattern of OsCRS2. (A) Relative expression levels of OsCRS2 in various tissues. (B-E) β-glucuronidase (GUS) staining of leaves (B), stems*

Discussion

The OsCRS2 leads to a decrease in chlorophyll content

The mutant *OsCRS2* was obtained from the SN9816 mutant library. The chlorophyll content of the mutant *OsCRS2* decreased, but the expression levels of genes involved in chlorophyll synthesis increased significantly, indicating that the abnormal chlorophyll content in the mutant *OsCRS2* was not caused by the obstruction of chlorophyll synthesis (Jenkins and Barkan, 2001). The most important reaction of O_2−is dismutation, which, under SOD or non-enzymatic conditions, is able to react with another O_2− molecule, resulting in oxidation of one of the molecules to oxygen and reduction of the second molecule to H_2O_2 (Lämmermann et al., 2019). The reduction in chlorophyll content may affect photosynthetic performance; however, the results of photosynthetic performance studies of some related mutants are quite different. Chlorophyll fluorescence parameters indicated that both qP and ΦPSII in the *OsCRS2* mutant were significantly increased, whereas NPQ was significantly decreased (LaRonde-LeBlanc et al., 2005). Although the photosynthetic efficiency of *OsCRS2* mutant was significantly increased, its yield was significantly decreased. This phenomenon may be due to the fact that the plant height, leaf length and leaf area index of *OsCRS2* mutant were significantly decreased, and the light energy fixed by *OsCRS2* was still significantly lower than that of the SN9816 (Mignolet-Spruyt et al., 2016). The reactive oxygen species content gradually increased with the severity of drought, the active oxygen scavenging system in plants was destroyed, and the dynamic balance between the production and elimination of free radicals was broken, resulting in unbalanced plant metabolism and oxidative damage to cells, accelerating lipid peroxidation in cell membranes. Malondialdehyde (MDA) accumulation can further affect the biofilm, resulting in the inactivation of other macromolecular structures and functions as well as membrane binding receptors and enzymes when the stress is more severe, causing severe cell damage, eventually forming a vicious cycle that leads to plant death (Mittler et al., 2004). Although the pigment antenna-size of the *OsCRS2* mutant was reduced, its net photosynthetic rate was significantly increased (Miyake et al., 2010). Thus, the smaller pigment antenna of mutant *OsCRS2* can still capture what is required for photosynthetic energy. The chloroplast structure was intact, indicating that the *OsCRS2* mutant had normal photosystem function. The increased RuBisCO activity ensured that the mutant *OsCRS2* had a high CO_2 fixation capacity. Rubisco, a rate-limiting enzyme in photosynthesis, is involved in the first step of carbon assimilation in photosynthesis, and Rubisco activity has a positive effect on the

http://www.aloki.hu ● ISSN 1589 1623 (Print) ● ISSN 1785 0037 (Online)
DOI: http://dx.doi.org/10.15666/aeer/2306_1115311167

CO_2 assimilation rate of plants (Mumm et al., 2011). The *OsCRS2* mutant improved electron transport efficiency by optimizing light energy utilization. Under normal conditions, ROS generation and scavenging of ROS reach balanced (Munekage et al., 2004). Antioxidants in the leaf defense mechanism were effectively activated and showed that the activity of antioxidant enzymes in leaves increased with the intensity and duration of drought. The results of this experiment showed that the change in antioxidant enzyme activity was in good agreement with the change in malondialdehyde content, because ROS accumulate continuously in plants under long-term stress, and malondialdehyde content MDA is produced in large quantities by activating antioxidant enzymes to combat the adverse reactions caused by oxidative stress. Antioxidant activity during rehydration remained high, indicating that plants retained some stress marks from previous droughts during recovery. Therefore, to adapt to adversity, plants must maintain a higher antioxidant enzyme activity (Carbonell-Caballero et al., 2015). The chlorophyll content and chlorophyll expression were significantly decreased in the *OsABC1K3* mutant. These results suggested that the *OsABC1K3* mutation affects chlorophyll synthesis, resulting in insufficient chlorophyll synthesis (Munekage et al., 2008). TUNEL assay also revealed massive cell apoptosis in OsABC1K3 mutant leaves. Thus, mutations in *OsABC1K3* cause ROS disorders in plants, leading to damage to intracellular nucleic acids (Chen et al., 2012). Under different degrees of drought stress conditions, the content of photosynthetic pigments in plants decreased significantly, the decrease in chlorophyll content was not conducive to chloroplast development, and the leaf color was yellow, white, and green. Lower photosynthetic efficiency and even lead to plant death. Chlorophyll plays an important role in light harvesting systems important role (Chen et al., 2019).

The increase in protective enzyme activity ensures the adaptability of the mutant OsCRS2 to high light intensity

Chlorophyll fluorescence is an important photosynthetic parameter that reflects the absorption and utilization of light energy by PSII (Wang et al., 2021). Generally, it is believed that a decrease in chlorophyll content may affect photosynthetic performance; however, the results of photosynthetic performance studies in some related mutants are quite different. Chlorophyll fluorescence parameters indicated that both qP and ΦPSII were significantly increased in the mutant *OsCRS2*, whereas NPQ was significantly decreased. Some studies have demonstrated a negative correlation between ΦPSII and NPQ (Herrera et al., 2000). It is generally believed that plant leaves tend to synthesize excessive chlorophyll to build larger antennae and capture and absorb more light energy than is required for photosynthesis (Ort et al., 2015). The absorbed excess light energy needs to be quenched through various photoprotective mechanisms to avoid ROS stress and photoinhibition; otherwise, it will lead to a decrease in light energy conversion efficiency (Kirst and Melis, 2014). The chlorophyll content and abundance of light-harvesting antenna proteins in the mutant *OsCRS2* were significantly reduced, resulting in a smaller pigment antenna size at the reaction center. Although the pigment antenna size of the mutant *OsCRS2* was reduced, its net photosynthetic rate was significantly increased. This phenomenon was also observed in the indica rice pe-1 mutant, where chlorophyll content decreased but photosynthesis was enhanced (Rao et al., 2019). Therefore, the smaller pigment antenna in mutant *OsCRS2* can still capture the light required for photosynthesis. The intact chloroplast structure indicates that the mutant *OsCRS2* has a normal photosystem function. The increase in RuBisCO activity ensures

http://www.aloki.hu ● ISSN 1589 1623 (Print) ● ISSN 1785 0037 (Online)
DOI: http://dx.doi.org/10.15666/aeer/2306_1115311167

that the mutant *OsCRS2* has a higher CO_2 fixation capacity. As the rate-limiting enzyme in photosynthesis, Rubisco participates in the first step of carbon assimilation, and Rubisco activity has a positive impact on the CO_2 assimilation rate of plants (Zhang et al., 2019). The mutant *OsCRS2* optimized the utilization of light energy and improved the efficiency of electron transfer. Under normal conditions, the generation and removal of ROS reach a balance and are harmless to plants (Zhang et al., 2017). However, ROS stress can lead to lipid peroxidation and the production of MDA in plants, and the MDA content is an important indicator of the degree of oxidative damage in cells (Toscano et al., 2016). The mutant *OsCRS2* has a smaller light-harvesting antenna size and higher light energy utilization efficiency, which can reduce the production of ROS, thereby reducing the peroxidation level of biological membrane lipids and lowering MDA content. The increase in CAT and POD activities also reflects the enhanced ability of mutant *OsCRS2* to remove ROS. On the other hand, reducing ROS levels and enhancing the activity of removal enzymes are of great significance for mutant *OsCRS2* to prevent ROS stress and photoinhibition under high light intensity. The increase in CAT activity can also enhance the activity of RuBisCO and improve the carbon assimilation capacity of mutant *OsCRS2* (Feng et al., 2020). Mutant *OsCRS2* has a lower NPQ, which can increase its electron transfer rate and light energy utilization efficiency by reducing heat dissipation. RuBisCO and FBA are important rate-limiting enzymes in plant photosynthesis. Increasing the activities of RuBisCO and FBA in the mutant *OsCRS2* can accelerate the photosynthetic rate and thereby improve light energy utilization efficiency. The results of this study show that mutant *OsCRS2* achieves a higher ΦPSII by increasing qP to better utilize light energy and reduce non-photochemical quenching. Although the photosynthetic efficiency of mutant *OsCRS2* was significantly improved, its yield showed a highly significant decrease. This phenomenon may be due to the highly significant decrease in plant height, flag leaf length, and leaf area index of the mutant *OsCRS2*, resulting in a significantly lower amount of light energy fixed by the plant compared to the wild-type SN9816.

Conclusion

These findings demonstrate significant interactions between to clarify the suitable and them SOD, which is a metalloenzyme that acts first when ROS levels are high. The antioxidant defense network SOD can convert O_2 -to H_2O_2, which can reduce the production of OH. CAT is a unique ROS-scavenging enzyme that rapidly breaks down H_2O_2 to produce water and oxygen, without any reduction. In addition to CAT, POD was also capable of scavenging excess H_2O_2, in the process, it oxidized phenolic compounds and generated phenoxy radicals. The increased malondialdehyde concentration proved that the *OsABC1K3* mutant cell membrane was damaged. peroxidase and superoxide dismutase levels were significantly increased in *OsABC1K3* mutants, but this did not restore them to normal levels. TUNEL assay also revealed massive cell apoptosis in *OsABC1K3* mutant leaves. Thus, mutations in *OsABC1K3* cause ROS disorders in plants, leading to damage to intracellular nucleic acids. The leaves of mutant *OsCRS2* exhibited a phenotype of low chlorophyll content, with a significant reduction in total chlorophyll content. However, there were no significant differences in the chloroplast ultrastructure. The mutant *OsCRS2* significantly enhanced the utilization efficiency of light energy, and the increase in RuBisCO activity strengthened the photosynthetic carbon assimilation capacity of the plant. By map-based cloning identification of *OsCRS2* candidate gene, a single-base mutation in its coding region led to the substitution of arginine amino acids

http://www.aloki.hu ● ISSN 1589 1623 (Print) ● ISSN 1785 0037 (Online)
DOI: http://dx.doi.org/10.15666/aeer/2306_1115311167

by glycine. The leaves of the transgenic complementary verification plants all returned to a normal green color, and the chlorophyll content and expression levels returned to normal. The subcellular localization of *OsCRS2* is chloroplasts, and it is mainly expressed in green tissues, such as leaves.

Acknowledgments. The authors are thankful to Special Project Funded by the Basic Research Business Expenses of the Chinese Academy of Agricultural Sciences (Y2023PT01) for financial support of this study.

Funding. The authors are thankful to Special Project Funded by the Basic Research Business Expenses of the Chinese Academy of Agricultural Sciences (Y2023PT01) for financial support of this study.

REFERENCES

[1] Busch, A. W., Montgomery, B. L. (2015): Interdependence of tetrapyrrole metabolism, the generation of oxidative stress and the mitigative oxidative stress response. – Redox Biol 4: 260-271.

[2] Carbonell-Caballero, J., Alonso, R., Ibañez, V., Terol, J., Talon, M., Dopazo, J. (2015): A phylogenetic analysis of 34 chloroplast genomes elucidates the relationships between wild and domestic species within the genus Citrus. – Mol Biol Evol 32: 2015-2035. https://doi.org/10.1093/molbev/msv082.

[3] Chen, L., Jia, H., Tian, Q., Du, L., Gao, Y., Miao, X., Liu, Y. (2012): Protecting effect of phosphorylation on oxidative damage of D1 protein by down-regulating the production of superoxide anion in photosystem II membranes under high light. – Photosynth Res 112: 141-148. https://doi.org/10.1007/s11120-012-9735-6.

[4] Chen, Z., Wang, H. C., Shen, J., Sun, F., Wang, M., Xu, C., Tan, B. C. (2019): PPR-SMR1 is required for the splicing of multiple mitochondrial introns, interacts with Zm-mCSF1, and is essential for seed development in maize. – J Exp Bot 70: 5245-5258. https://doi.org/10.1093/jxb/erz295.

[5] Cui, H., Ding, Z., Zhu, Q., Wu, Y., Qiu, B., Gao, P. (2021): Comparative analysis of nuclear, chloroplast, and mitochondrial genomes of watermelon and melon provides evidence of gene transfer. – Sci Rep 11: 1595. https://doi.org/10.1038/s41598-020-79626-1.

[6] Feng, B. H., Li, G. Y., Islam, M., Fu, W. M., Zhou, Y. Q., Chen, T. T., Tao, L. X., Fu, G. F. (2020): Strengthened antioxidant capacity improves photosynthesis by regulating stomatal aperture and ribulose-1,5-bisphosphate carboxylase/oxygenase activity. – Plant Science 290: 110245.

[7] Herrera, A., Fernández, M. D., Taisma, M. A. (2000): Effects of drought on CAM and water relations in plants of Peperomia carnevalii. – Annals of Botany 86(3): 511-517.

[8] Hu, T., Chong, Y., Lu, S., Wang, R., Qin, H., Silva, J., Kitamura, E., Chang, C. S., Hawthorn, L., Cowell, J. K. (2018): miR-339 promotes development of stem cell leukemia/lymphoma syndrome via downregulation of the BCL2L11 and BAX proapoptotic genes. – Cancer Res 78: 3522-3531. https://doi.org/10.1158/0008-5472.CAN-17-2919.

[9] Kirst, H., Melis, A. (2014): The chloroplast signal recognition particle (CpSRP) pathway as a tool to minimize chlorophyll antenna size and maximize photosynthetic productivity. – Biotechnology Advances 32(1): 66-72.

[10] Kumar, S., Singh, B. (2009): Effect of water stress on carbon isotope discrimination and Rubisco activity in bread and durum wheat genotypes. – Physiol Mol Biol Plants 15: 281-286. https://doi.org/10.1007/s12298-009-0031-1.

[11] Lämmermann, N., Schmid-Michels, F., Weißmann, A., Wobbe, L., Hütten, A., Kruse, O. (2019): Extremely robust photocurrent generation of titanium dioxide photoanodes bio-

http://www.aloki.hu ● ISSN 1589 1623 (Print) ● ISSN 1785 0037 (Online)
DOI: http://dx.doi.org/10.15666/aeer/2306_1115311167

sensitized with recombinant microalgal light-harvesting proteins. – Sci Rep 9: 2109. https://doi.org/10.1038/s41598-019-38660-9.

[12] LaRonde-LeBlanc, N., Wlodawer, A. (2005): A family portrait of the RIO kinases. – J Biol Chem 280: 37297-37300. https://doi.org/10.1074/jbc.R500009200.

[13] Lin, Y. P., Shen, Y. Y., Shiu, Y. B., Charng, Y. Y., Grimm, B. (2022): Chlorophyll dephytylase 1 and chlorophyll synthase: a chlorophyll salvage pathway for the turnover of photosystems I and II. – Plant J 111: 979-994.

[14] Ma, J. J., Yang, S. X., Wang, D. M., Tang, K. Q., Feng, X. X., Feng, X. Z. (2020): Genetic mapping of a light-dependent lesion mimic mutant reveals the function of coproporphyrinogen III oxidase homolog in soybean. – Front. Plant Sci. 11: 557.

[15] Mignolet-Spruyt, L., Xu, E., Idänheimo, N., Hoeberichts, F. A., Mühlenbock, P., Brosché, M., Van Breusegem, F., Kangasjärvi, J. (2016): Spreading the news: subcellular and organellar reactive oxygen species production and signalling. – J Exp Bot 67: 3831-3844. https://doi.org/10.1093/jxb/erw080.

[16] Mittler, R., Vanderauwera, S., Gollery, M., Van Breusegem, F. (2004): Reactive oxygen gene network of plants. – Trends Plant Sci 9: 490-498. https://doi.org/10.1016/j.tplants.2004.08.009.

[17] Miyake, C. (2010): Alternative electron flows (water-water cycle and cyclic electron flow around PSI) in photosynthesis: molecular mechanisms and physiological functions. – Plant Cell Physiol 51: 1951-1963. https://doi.org/10.1093/pcp/pcq173.

[18] Mumm, P., Wolf, T., Fromm, J., Roelfsema, M. R., Marten, I. (2011): Cell type-specific regulation of ion channels within the maize stomatal complex. – Plant Cell Physiol 52: 1365-1375. https://doi.org/10.1093/pcp/pcr084.

[19] Munekage, Y., Hashimoto, M., Miyake, C., Tomizawa, K., Endo, T., Tasaka, M., Shikanai, T. (2004): Cyclic electron flow around photosystem I is essential for photosynthesis. – Nature 429: 579-582. https://doi.org/10.1038/nature02598.

[20] Munekage, Y. N., Genty, B., Peltier, G. (2008): Effect of PGR5 impairment on photosynthesis and growth in Arabidopsis thaliana. – Plant Cell Physiol 49: 1688-1698. https://doi.org/10.1093/pcp/pcn140.

[21] Niazian, M., Sadat-Noori, S. A., Tohidfar, M., Mortazavian, S. M. M., Sabbatini, P. (2021): Betaine aldehyde dehydrogenase (BADH) vs. flavodoxin (Fld): two important genes for enhancing plants stress tolerance and productivity. – Front Plant Sci 12: 650215. https://doi.org/10.3389/fpls.2021.650215.

[22] Nie, L., Cui, Y., Wu, L., Zhou, J., Xu, Z., Li, Y., Li, X., Wang, Y., Yao, H. (2019): Gene losses and variations in chloroplast genome of parasitic plant Macrosolen and phylogenetic relationships within Santalales. – Int J Mol Sci 20: 5820. https://doi.org/10.3390/ijms20225820.

[23] Nikkanen, L., Rintamäki, E. (2019): Chloroplast thioredoxin systems dynamically regulate photosynthesis in plants. – Biochem J 476: 1159-1172. https://doi.org/10.1042/BCJ20180612.

[24] Nishikawa, Y., Yamamoto, H., Okegawa, Y., Wada, S., Sato, N., Taira, Y., Sugimoto, K., Makino, A., Shikanai, T. (2012): PGR5-dependent cyclic electron transport around PSI contributes to the redox homeostasis in chloroplasts rather than CO2 fixation and biomass production in rice. – Plant Cell Physiol 53: 2117-2126. https://doi.org/10.1093/pcp/pcs154.

[25] Noctor, G., Reichheld, J. P., Foyer, C. H. (2018): ROS-related redox regulation and signaling in plants. – Semin Cell Dev Biol 80: 3-12. https://doi.org/10.1016/j.semcdb.2017.07.013.

[26] Ort, D. R., Merchant, S. S., Alric, J., Barkan, A., Blankenship, R. E., Bock, R., Croce, R., Hanson, M. R., Hibberd, J. M., Long, S. P., Yuan, J. S., Zhu, X. G. (2015): Redesigning photosynthesis to sustainably meet global food and bioenergy demand. – Proceedings of the National Academy of Sciences of the United States of America 112(28): 8529-8536.

[27] Rao, Y., Xu, N., Li, S., Hu, J., Jiao, R., Hu, P., Lin, H., Lu, C., Lin, X., Dai, Z., Zhang, Y., Zhu X., Wang, Y. (2019): PE- 1, encoding heme oxygenase 1, impacts heading date and

http://www.aloki.hu ● ISSN 1589 1623 (Print) ● ISSN 1785 0037 (Online)
DOI: http://dx.doi.org/10.15666/aeer/2306_1115311167

chloroplast development in rice (Oryza sativa L.). – Journal of Agricultural and Food Chemistry 67(26): 7249-7257.

[28] Rühle, T., Dann, M., Reiter, B., Schünemann, D., Naranjo, B., Penzler, J. F., Kleine, T., Leister, D. (2021): PGRL2 triggers degradation of PGR5 in the absence of PGRL1. – Nat Commun 12: 3941. https://doi.org/10.1038/s41467-021-24279-3.

[29] Schöttler, M. A., Thiele, W., Belkius, K., Bergner, S. V., Flügel, C., Wittenberg, G., Agrawal, S., Stegemann, S., Ruf, S., Bock, R. (2017): The plastid-encoded PsaI subunit stabilizes photosystem I during leaf senescence in tobacco. – J Exp Bot 68: 1137-1155. https://doi.org/10.1093/jxb/erw471.

[30] Shikanai, T., Munekage, Y., Shimizu, K., Endo, T., Hashimoto, T. (1999): Identification and characterization of Arabidopsis mutants with reduced quenching of chlorophyll fluorescence. – Plant Cell Physiol 40: 1134-1142. https://doi.org/10.1093/oxfordjournals.pcp.a029490.

[31] Toscano, S., Farieri, E., Ferrante, A., Romano D. (2016): Physiological and biochemical responses in two ornamental shrubs to drought stress. – Frontiers in Plant Science 7: 645.

[32] Wang, S., Zheng, J., Wang, Y., Yang, Q., Chen, T., Chen, Y., Chi, D., Xia, G., Siddique, K. H. M., Wang T. (2021): Photosynthesis, chlorophyll fluorescence, and yield of peanut in response to biochar application. – Frontiers in Plant Science 12: 650432.

[33] Xu, C. H., Zhu, Q. J., Chen, J. H., Shen, L. G., Yi, X. H., Huang, Z. H., Wang, W., Chen, M., Kuang, T., Shen, J. R., Zhang, X., Han, G. Y. (2021): A unique photosystem I reaction center from a chlorophyll d-containing cyanobacterium Acaryochloris marina. – J. Integr. Plant Biol 63: 1740-1752.

[34] Zhang, L., Hu, T., Amombo, E., Wang, G., Xie, Y., Fu J. (2017): The alleviation of heat damage to photosystem II and enzymatic antioxidants by exogenous spermidine in tall fescue. – Frontiers in Plant Science 8: 1747.

[35] Zhang, T., Feng, P., Li, Y., Yu, P., Yu, G., Sang, X., Ling, Y., Zeng, X., Li, Y., Huang, J., Zhang, T., Zhao, F., Wang, N., Zhang, C., Yang, Z., Wu, R., He, G. (2018): VIRESCENT-ALBINO LEAF 1 regulates leaf colour development and cell division in rice. – J Exp Bot 69: 4791-4804. https://doi.org/10.1093/jxb/ery267.

[36] Zhang, Y., Zhou, Y., Sun, Q., Deng, D., Liu, H., Chen, S., Yin, Z. (2019): Genetic determinants controlling maize rubisco activase gene expression and a comparison with rice counterparts. – BMC Plant Biol 19: 351. https://doi.org/10.1186/s12870-019-1950-4.

[37] Zhao, Y., Xu, W., Wang, L. J., Han, S., Zhang, Y. Z., Liu, Q. Z., Liu, B. S., Zhao, X. Y. (2022): A maize necrotic leaf mutant caused by defect of coproporphyrinogen III oxidase in the porphyrin pathway. – Genes 13: 272.

[38] Zhou, F., Karcher, D., Bock, R. (2007): Identification of a plastid intercistronic expression element (IEE) facilitating the expression of stable translatable monocistronic mRNAs from operons. – Plant J 52: 961-972. https://doi.org/10.1111/j.1365-313X.2007.03290.

http://www.aloki.hu ● ISSN 1589 1623 (Print) ● ISSN 1785 0037 (Online)
DOI: http://dx.doi.org/10.15666/aeer/2306_1115311167